CFD ANALISYS OF AN INDUSTRIAL GAS TURBINE COMBUSTION CHAMBER

Thiago Koichi Anzai, Carlo Eduardo Fontes, Karolline Ropelato {anzai, carlos.fontes, ropelato}@esss.com.br
Engineering Simulation and Scientic Software (ESSS), Ltda. Rio de Janeiro, BRAZIL

Luís Fernando Figueira da Silva, Luis Enrique Alva Huapaya {luisfer, luisalva}@esp.puc-rio.br
Departament of Mechanical Engineering, Pontifícia Universidade Católica do Rio de Janeiro, Rio de Janeiro, BRAZIL

Abstract. *The determination of pollutant emissions from gas turbine combustors is a crucial problem which cannot be fully tackled experimentally, since a study of all possible operation conditions is economically unfeasible. As direct numerical simulation (DNS) of industrial combustors is also beyond reach of the foreseeable computational resources, models must be used for the analysis of such issue. This work presents the results obtained for an industrial gas turbine combustion chamber using computational fluid dynamics (CFD). The model used contains an ad-hoc parameter for which a new formulation is proposed. The influence of this new formulation is examined both in terms of the flowfield structure and the combustion stabilization mechanism.*

Keywords*: Combustion, Gas turbine, Computational Fluid Dynamics*.

1. INTRODUCTION

The accurate determination of pollutant emission from gas turbine combustors is a crucial problem in situations when such equipment is subject to long periods of operation away from the design point. In such operating conditions, the flowfield structure may also drastically differ from the design point one, leading to the presence of undesirable hot spots or combustion instabilities, for instance. A priori experiments on all possible operation conditions is economically unfeasible, therefore, models that allow for the prediction of combustion behavior in the full operation range could be used to instruct power plant operators on the best strategies to be adopted. Since the direct numerical simulation of industrial combustors is beyond reach of the foreseeable computational resources, simplified models should be used for such purpose.

This works presents the results of the application to an industrial gas turbine combustion chamber of the CFD technique to the prediction of the reactive flowfield. This is the first step on the coupling of reactive CFD results with detailed chemical kinetics modeling using chemical reactor networks (Huapaya et al. 2010, Orbegoso et al. 2009) toward the goal of accurately predicting pollutant emissions. The CFD model considers the detailed geometrical information of such a combustion chamber and uses actual operating conditions, calibrated via an overall gas turbine thermodynamicall simulation, as boundary conditions (Orbegoso et al., 2009). This model retains the basic information on combustion staging, which occurs both in diffusion and lean premixed modes.

The turbulence has been modeled using the SST-CC model (Menter, 1994), which is characterized by a well established regime of accurate predictive capability. Combustion and turbulence interaction is accounted for by using the Zimont et al. (2001) model, which makes use of on empirical expression for the turbulent combustion velocity for the closure of the progress variable transport equation. A high resolution scheme is used to solve the advection terms of the momentum equation. Numerical results of turbulent partially premixed combustion in gas turbine combustion chamber operating at full load conditions are discussed. The following presentation is divided in three main parts. First, the mathematical formulation is briefly introduced, with emphasis on the combustion model parameters and boundary conditions used. Then, the structure of the reactive flow field is discussed in terms of the scalar fields characteristic of the combustion process. Finally, the results are examined in order to unveil the underlying flame brush stabilization mechanism.

2. MATHEMATICAL FORMULATION AND BOUNDARY CONDITIONS

2.1. Zimont Model

With the purpose of describing the flowfield resulting from the turbulent combustion process that arises within the combustion chamber, the classical Reynolds Averaged Navier Stokes transport equations are solved for momentum transport (Poinsot and Veynante, 2005; Pope, 2000). Even if the modeled flowfield will be shown to be characterized by large scale structures and strong rotation, turbulence in modeled by the eddy-viscosity based SST-CC model (Menter, 1994). This is justified on the basis of the known model deficiencies, such as the inability to describe turbulence increase through a flame brush, but also on the well proven capacity to reasonably describe turbulent transport. These equations are solved using the standard options of the ANSYS CFX 12.1 computer code (CFX, A. 2009). Combustion is modeled using a partially premix model, which is standard in this code, and is based on the Zimont et al. (1977)

premixed combustion model. Since this model exhibits empirical constants which value is subject to a parametrical study herein, its main ideas will be presented here.

This model solves an equation for the reaction progress variable, c the reaction progress variable,

$$\partial(\rho c)/\partial t + \partial(\rho \tilde{u}_j c)/\partial x_j = \partial[(\rho D+\mu_t/\sigma_c)\,\partial c/\partial x_j]/\partial x_j + S_T\,|\partial c/\partial x_j|, \quad (1)$$

where the μ_t turbulent viscosity, and σ_c is Schmidt number, c represents a non dimensional temperature (Borghi e Champion, 2000), ρ is the density, $\tilde{u}_j$ velocity component (j =1,2,3) and D is the molecular turbulent diffusion coefficient.

For turbulent flow, the effective or turbulent burning velocity s_T differs from the laminar flame speed, s_L. Typically turbulence will increase the burning velocity, because wrinkling of the flame front results in an increased effective flame surface (Driscoll 2008, Zimont et al. 1977). At very high turbulence, the opposite effect may occur, leading to a decrease in the effective burning velocity because of local extinction. A model is thus required to describe the turbulent burning relative to the unburnt fluid. The clousure developed by Zimont et al. (1998), is used for the turbulent burning velocity:

$$S_T = G\,A\,u'^{3/4}\,Da^{1/4}, \quad (2)$$

where G is a stretching factor, A, is a modeling coefficient that has the "universal" value A=0.5, the local turbulent velocity intensity is u', and Da is the Damköhler number. The stretching factor, G, accounts for reduction of the flame velocity due to large strain rate (large dissipation rate of the turbulent kinetic energy). This effect is modeled in terms of the probability for turbulence eddy dissipation, ε, being larger than a critical value ε_{cr}. For $\varepsilon > \varepsilon_{cr}$, flamelet extinction takes place, while for $\varepsilon < \varepsilon_{cr}$, the stretching effect is ignored completely. Assuming a lognormal distribution for ε, the stretching factor is given by:

$$G = (1/2)\mathrm{erfc}\,[(-1/\sqrt{(2\sigma)})(\ln(\varepsilon_{cr}/\varepsilon)+(\sigma/2)], \quad (3)$$

where erfc denotes the complementary error function and $\sigma = \mu_{str}\,\ln(Re^{3/4})$ is the standard deviation of the distribution of ε, with μ_{str} being an empirical model coefficient (μ_{str}=0.28).

The critical dissipation rate, ε_{cr}, is computed from a prescribed critical extinction factor, g_{cr} and the kinematic viscosity of the fluid, ν, (Zimont , 1998), (Zimont, 1999) and (Zimont, 2001) according to:

$$\varepsilon_{cr} = 15\,\nu\,g_{cr}^{2}. \quad (4)$$

In this model the Damköhler number is related to speed the freely propagating laminar flame speed, s_L, (Zimont, 1998), which may be determined from by experiments or calculations. In this work S_L was determined as a function of equivalence ratio, temperature and pressure using the premix code (Kee et al. 1985, 1989) together with a detailed description of the combustion chemistry using GRI 3.0 mechanism (Smith, 1999) for methane and air mixtures. The results of such a computations are given in figure 1.

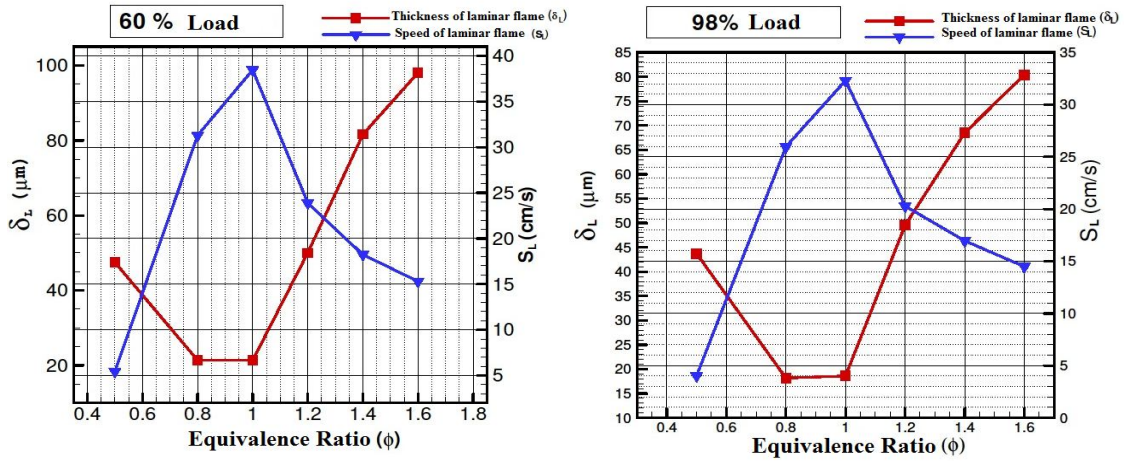

Figure 1: Laminar flame speed and reaction zone thickness as a function of equivalent ratio, corresponding to different turbine loads; 60% load (T=661 K, p=1.1 Mpa); 98% load (T=661 K, p=1.4 Mpa).

The determination of the critical extinction factor is less obvious. An original methodology is proposed here for its determination in which the structure of the laminar premixed flame is considered as a function of the equivalence ratio of the mixture and for different values of pressure and temperature upstream to the flame.

It is assumed that flame extinction occurs once the reaction zone has been sufficiently disturbed by turbulence, thus,

$$g_{cr}=C_g S^1_L/\delta_R, \tag{5}$$

where δ_R is the thickness of the reaction zone and S^1_L is the flame speed with respect to the burned gases, $S^1_L=S_L\rho_0/\rho_1$; C_g is a model constant which influence on the results will be investigated. The definition of δ_R used is based on the detailed computations results of premixed flames, such as those shown in figure 1.

Figure 2 which shows the rate of heat release by the flame as a function of distance for three values of equivalence ratio, allows to verify that the maximum value of heat release, Qmax, occurs at the vicinity of the burned gases.

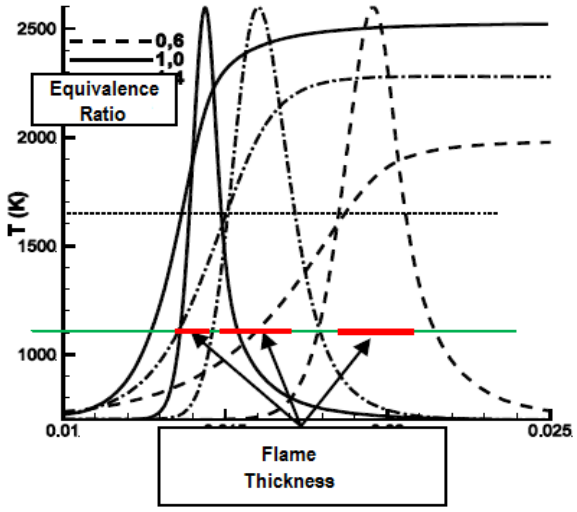

Figure 2: Evolution of temperature and rate of heat release on laminar premixed flames for three values of equivalence ratio, 0.6; 1; 1.4 .

This, the thickness of the zone of reaction is defined as

$$\delta_R= x_2(Q_{max}/2)-x_1(Q_{max}/2), \tag{6}$$

which is sketched in figure 2, the evolution of δ_R with equivalence ratio is given in figure 1.

The computed dependency of the critical extinction factor with the equivalence ratio is shown in figure 3. This figure suggests that smaller values of g_{cr} are required to extinguish flames in either lean or rich mixtures, when compared to stoichiometric ones. Note, also, the large variation of g_{cr}, which allows to understand the range of values recommended by Zimont (2001), between 10,000 and 100,000.

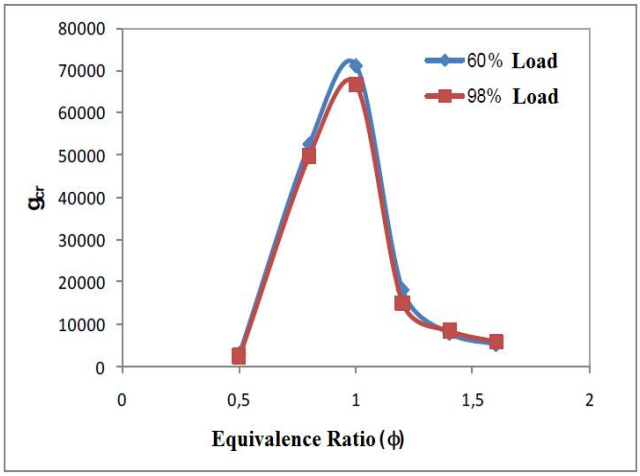

Figure 3: Relation between the critical extinction factor the equivalent ratio of the mixture for two gas turbine loads.

2.2. Combustion Chamber Layout

Figure 4 shows a cross sectional view of the gas turbine combustion chamber considered in this work. In this figure the air flows from right to left at the outside of the chamber where it is mixed with 7% of fuel (natural gas) in "stage c". Then, the mixture turns 180° and, upon passing different swirling vanes, enters the combustion chamber where the fuel is injected.

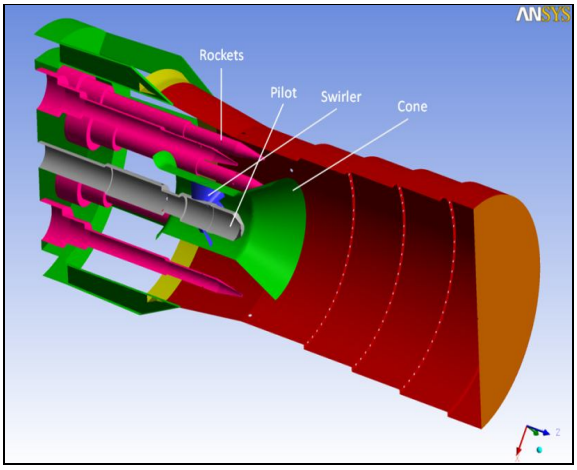

Figure 4: Cut-off view of the combustion chamber.

Within the chamber, fuel injection is performed by a central mast (dubbed pilot stage), which comprises eight (2 mm diameter) orifices inclined with respect to the chamber central axis, and by eight peripheral masts, each with four orifices (3 mm diameter) that inject fuel normal to the flow direction, and are reffered to as stages A&B. The pilot stage, which is responsible for combustion stabilization, is separated from stages A&B by a conical surface.

The swirling vanes of stages A&B impart a mild rotation movement to the flow, whereas the orientation of the pilot stage swirling vanes is such that a strong flow rotation results.

The combustion chamber thermal protection is partly guaranteed by four series of cooling air orifices, which are arranged in recesses of the combustion chamber wall and that lead to the formation of an adjacent fresh air film.

2.3. Boundary Conditions

The present study considers the operation of the combustion chamber at base load conditions (98% load). These conditions correspond to a total mass flow rate of fuel and air of 163 g/s and 5.152kg/s, respectively. Air and fuel enter the computational domain at temperatures of 661K and 411 K, respectively, the pressure at the combustion chamber is 1.4 MPa. The fuel flow is distributed as follows: 10% is premixed with air in stage C upstream to the swirling vanes, 8.5% is evenly distributed by the eight pilot stage orifices, the remainder is injected via each of the four orifices of the eight stage A&B masts. Note that previous studies (Orbegoso et al. 2009) have indicated that 9% of the total air mass flow rate is used downstream to the combustion chamber for dilution purposes. The mass flow rates in the different injection stages are prescribed according to table 1.

The nonreactive case turbulent field was used as initial condition for the case with combustion details of the computational mesh may be found elsewhere. (Huapaya et al. 2010). All boundary conditions are classical, i.e., walls are adiabatic, no slip surfaces, temperature, composition, mass flow rate and turbulent quantities are imposed at the inflow boundaries and pressure is extrapolated at the exit boundary. Symmetry conditions are used in the faces of the ¼-sector of the combustion chamber used in the computations.

Table 1. Conditions of reactant supply of the stages at 98% load.

Pressure (kPa)		1446
Fuel	**StageA&B(kg/s)**	0.132
	Pilot Stage (kg/s)	0.014
	Stage C (kg/s)	0.017
	Temperature (K)	411
Air	**Plenum (kg/s)**	5.152
	Temperature (K)	661

.

3. STRUCTURE OF THE REACTIVE FLOW

In this section the influence of the model constant C_g [Eq. (5)] on the structure of the reactive flow field will be examined in terms of the evolution of the equivalence ratio and the reaction progress variable, which are the transported parameters of the combustion model.

3.1. Equivalence ratio field

In order to characterize fuel/air mixing the equivalence ratio field is shown in figure 5 for different values of C_g = 1, 10 and 100. Note that, since this combustion chamber is expected to operate mostly in the lean premixed mode, only lean values of equivalence ratio are shown. Concerning the flowfield downstream to the pilot stage at the central portion of the combustion chamber, the influence of C_g is not perceptible. On the other hand, the mixing flowfield downstream to stages A&B is somewhat influenced by the choice of C_g immediately downstream to the fuel injection masts. Indeed, as C_g is increased a larger segregation between fuel and air is observed. This indicates that the combustion process at the stages A&B influences the scalar mixing field.

In order to further characterize the mixing field, figure 6 depicts the stoichiometric iso-surface in the case where C_g=100. These iso-surfaces, which have been coloured by temperature, show that, at the peripheral stages, mixing proceeds without reaction until stoichiometric conditions are attained. On the other hand, in the pilot stage, the intense turbulent stirring leads to mixing between combustion products and reactants, thus indicating that stirred reactor conditions prevail.

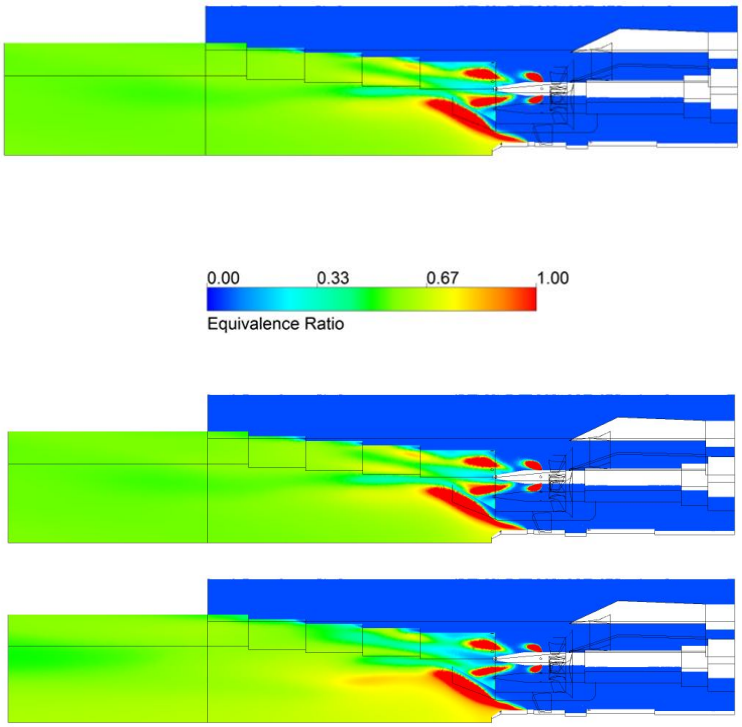

Figure 5: Equivalence ratio distribution in a longitudinal cross-section of the combustion chamber for: C_g = 1, 10 and 100 (top to bottom).

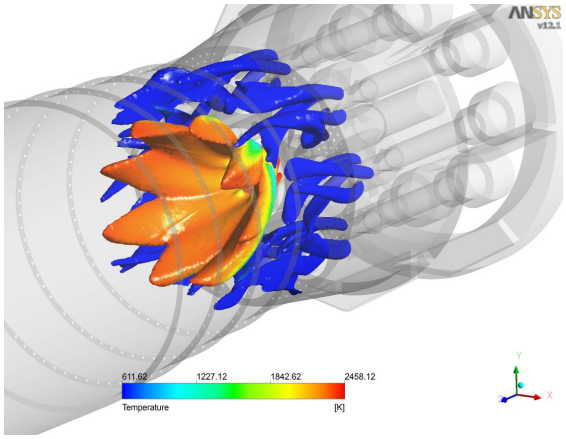

Figure 6: Isosurface of stoichiometric mixture fraction coloured by temperature for the case with C_g = 100.

3.2. Progress variable field

This progress variable field is expected to be strongly influenced by the value of C_g. This is indeed the case, as may be verified in figure 7, which shows c fields for different values of C_g. Note that the value of c is directly linked to the temperature, c=0 represents the fresh unburned gases and c=1 the fully burned state.

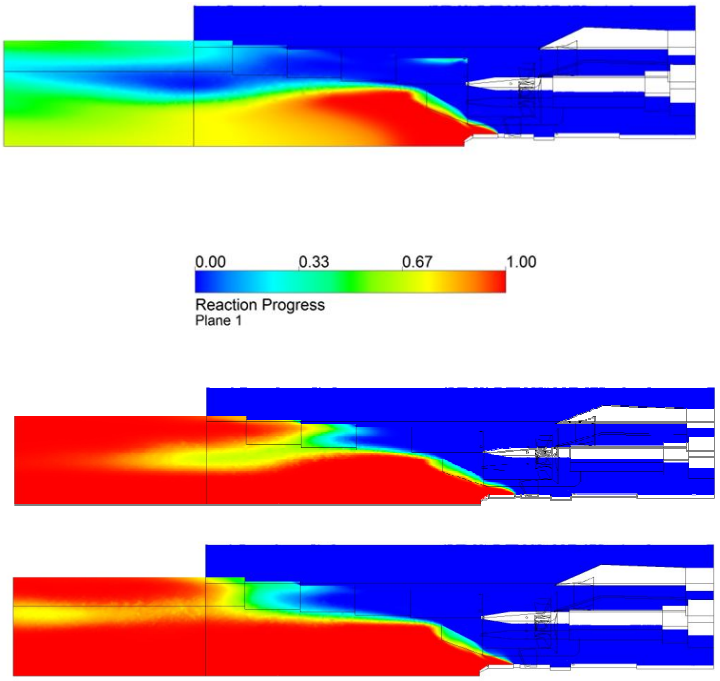

Figure 7: Progress variable distribution in a longitudinal cross-sectional plane to the combustion chamber for C_g = 1; 10 and 100 (top to bottom).

This figure shows the cross-sectional extension of the burned region increases significantly with the increase of C_g from 1 to 10. In particular, when C_g = 1, combustion of the stages A&B mixture is found to begin near the exit of the combustion chamber, downstream to the cooling orifices, which is evidently incorrect. Furthermore, incomplete combustion downstream to the pilot stage is calculated which, again, is not reasonable for the present full load operating condition. When C_g = 10 and 100 the lean premixed flame front is stabilized inside the combustor basket, as it could be expected.
Note, however, that the use of a single cross-section plane to analyze the obtained results does not allow to observe the computed 3D large scale wrinkling effect of the flame brush. Indeed, figure 8, which shows the field of c at the exit of the combustion chamber, clearly shows that the amount of burned gases increase with C_g.

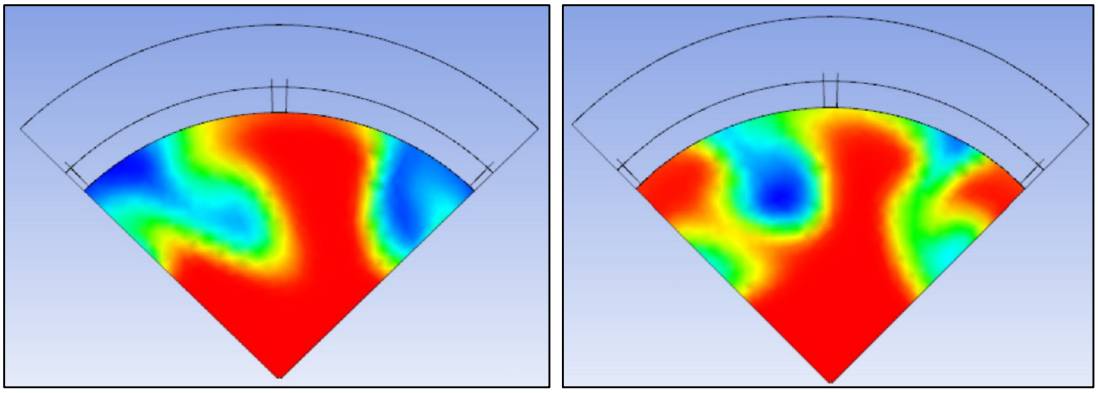

Figure 8: Fields of c in a transversal cross-sectional plane at the exit of the combustion chamber for C_g = 10 and 100 (left to right).

4. FLAME STABILIZATION MECHANISM

In order to examine the outcome of the flame stabilization mechanism embedded within the Zimont model, figures 9 and 10 depict, for different values of C_g, the turbulent flame speed S_T and the ratio $\varepsilon/\varepsilon_{cr}$. The first of this quantities express the possibility of the flame brush to propagate with a given speed which must equilibrate the local flow velocity for a stable flame to be possible. For the sake of completeness, figure 11 shows the modulus of the velocity in the case C_g = 1; 10 and 100.

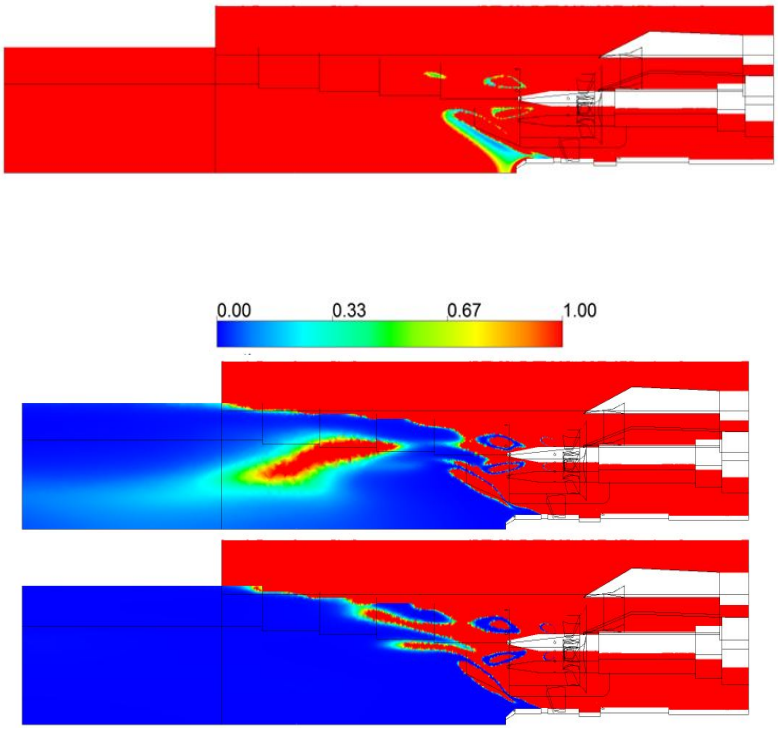

Figure 9: Ratio $\varepsilon/\varepsilon_{cr}$, in a longitudinal cross-sectional plane to the combustion chamber for C_g = 1; 10 and 100 (top to bottom).

The $\varepsilon/\varepsilon_{cr}$ ratio actually controls the quenching of the flame, which occurs when $\varepsilon/\varepsilon_{cr}>1$. Therefore, if $\tilde{u} \geq S_T$ a flame brush may be stabilized, but its existence is warranted only if, simultaneously, $\varepsilon/\varepsilon_{cr}<1$.

Indeed, figure 10 shows that for C_g = 1 small values of S_T exist at the periphery of the combustion chamber and downstream to the pilot stage, when compared to those computed for C_g = 10 or 100. Based on this figure, it may be concluded that it is more likely for a turbulent flame to be found in cases where C_g = 10 or 100 than that of C_g = 1. The velocity values depicted in figure 11 indicate that, at the periphery of the combustion chamber, $\tilde{u} \geq S_T$, which could lead to the presence of a flame brush inclined with respect to the flow only.

Examining now figure 10, the extreme influence of the choice of C_g on $\varepsilon/\varepsilon_{cr}$ may be verified. Indeed, when C_g = 100, the turbulent flame could be stabilized almost anywhere within the combustion chamber, since $\varepsilon/\varepsilon_{cr}<1$ regions prevails. In this situation, the flame position is the result of a pure kinematic balance of flame versus flow velocity. The opposite trend is observed for C_g = 1, again, note that a representation based on this cross-section only does not allow for a complete picture of the flow field. The case of C_g = 10 is an intermediate situation where the flow field alters quenching and stabilizing regions.

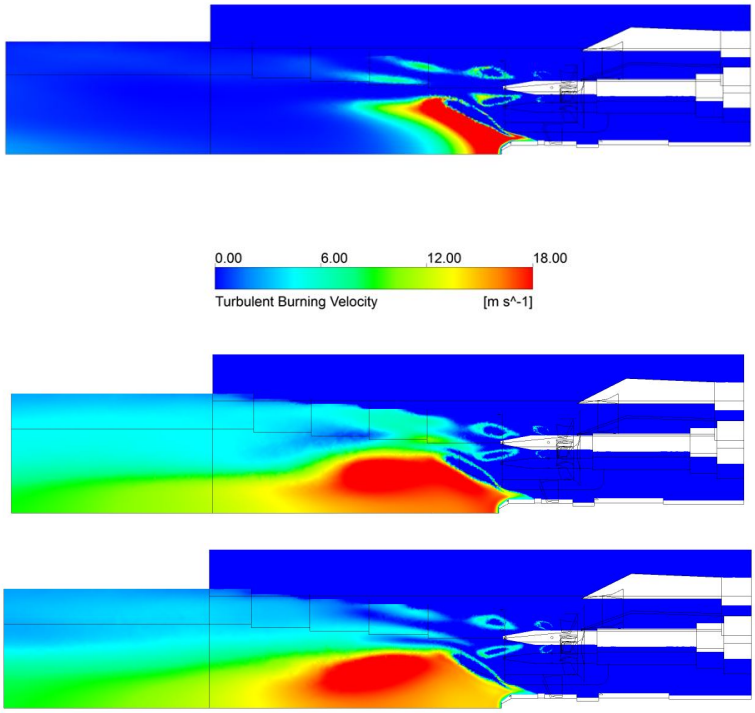

Figure 10: Turbulent flame velocity distribution in a longitudinal cross-sectional plane to the combustion chamber for C_g = 1; 10 and 100 (top to bottom).

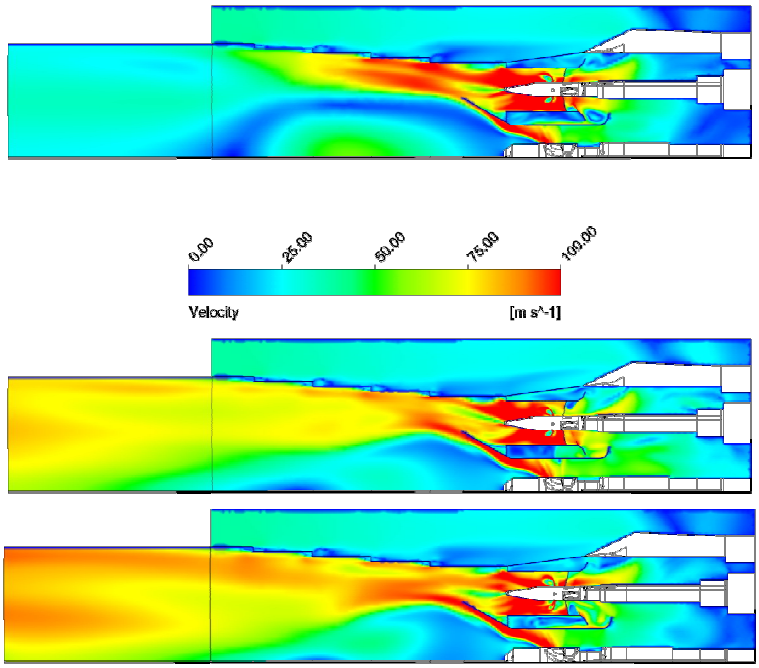

Figure 11: Modulus of the velocity in a longitudinal cross-sectional plane to the combustion chamber for C_g = 1; 10 and 100 (top to bottom).

5. FINAL REMARKS

This work presented the results of a parametrical analysis of the influence of the choice of a turbulent combustion model parameter on the computed flowfield of a gas turbine combustion chamber. A new functional expression for such a model parameter, which represents extinction of the flame brush by turbulent eddies, was proposed based on laminar flames computed with detailed chemistry. Since this expression involves an ad-hoc constant, the parametrical analysis performed involved varying its value by three orders of magnitude.

The computed results allow to examine the averaged flowfield within the combustion chamber, which indicates that a plausible value for such a constant is $C_g = 10$. The exact value should be determine by comparing the model results to will characterized experiments representative of premixed and partially premixed combustion, such as those of Besson et al. (2000).

6. REFERENCE

Besson M., Bruel P., Champion J. L., and Deshaies B., 2000, "Experimental Analysis of Combusting Flows Developing Over a Plane – Symmetric Expansion", Journal Thermophys. Heat Transfer, Vol. 14, pp. 56 – 67.

Borghi R., Champion M., 2000, "Modélisation et Théorie des Flammes", Editions Technip, Paris-France, 402 p.

CFX. A., 2009, Theory Documentation V.12.

Driscoll J. F., 2008, "Turbulent Premixed Combustion Flamelet Structure and its Effect on Turbulent Burning Velocities", Progress in Energy and Combustion Science, Vol. 34, pp. 91 – 134.

Huapaya, L. E. A., Figueira da Silva, L. F., Souza, J. Z., Ribeiro, D. C., Anzai, T., Ropelato, K., and Fontes, C. E., 2010, "Combined CFD and Reactor Network Modeling of an Industrial Gas Turbine Combustor", In: 10th International Conference on Combustion and Energy Utilization, Mugla, Turkeg.

Kee R. J., Grear J. F., Smook M. D. and Miller, J. A., 1985, "PREMIXED: A Fortran Program for Modeling Steady Laminar One-Dimensional Premixed Flame", Report No. SANS85-8240, Sandia National Laboratories.

Kee R. J., Rupley F. M. and Miller J. A., 1989, "Chemkin-II. A Fortran Chemical Kinetics Package for the Analysis of Gas-Phase Chemical Kinetics", Sandia Report No. SANS89-8009B, Sandia National Laboratories.

Menter, F., 1994, "Two-Equation Eddy-Viscosity Turbulence Models for Engineering Applications", AIAA Journal, 32(8), pp. 1598-1605.

Orbegoso, E. M., Romeiro, C. D., Ferreira, S. B., Figueira da Silva, L. F., 2009, "Emissions and Thermodynamic Performance Simulation of an Industrial Gas Turbine", In: 45th AIAA/ASME/SAE/ASEE Joint Propulsion Conference & Exhibit, 2009, Denver. Washington : American Institute of Aeronautics and Astronautics, Vol. 45. pp. 1-28.

Poinsot T., Veynante D., 2005 "Theoretical and Numerical Combustion", second edition, 519 p.

Pope, S. B., 2000, "Turbulent Flows", Cambridge University Press.

Smith, G. P., 1999, Source: Gri-Mech Website: http://www.me.berkeley.edu/gri-mech.

Zimont, V. L., 1977, "On the Calculation of the Partially Premixed Turbulent Combustion of Gases", In: Proceedings of Combustion of Heterogeneous and Gas Systems, USSR Academy of Science, Chernogolovka (in Russian) pp. 76-80.

Zimont, V. L., 1998, "An Efficient Computational Model for Premixed Turbulent Combustion at High Reynolds Numbers Based on a Turbulent Flame Speed Closure", Journal Engineering for Gas Turbines and Power, Vol. 120, pp. 526-532.

Zimont, V. L., 1999, "Gas Premixed Combustion at High Turbulence". Proceedings of the Mediterranean Combustion Symposium, Vol. 1, pp. 1155-1165.

Zimont, V. L., Biagioli, F., Syed K., 2001, "Modelling Turbulent Premixed Combustion in the Intermediate Steady Propagation Regime", Progress in Computational Fluid Dynamics , Vol. 1, pp. 14-28.